VOLUME 270 15 APRIL 2014 ISSN 0029-5493

Nuclear Engineering and Design

An International Journal devoted to all aspects of Nuclear Fission Energy

Engineering Mechanics
Reliability of double-wall containment against the impact of hard projectiles
N.A. Siddiqui, B.M.A. Khateeb, T.H. Almusallam and H. Abbas 143
Thermal stress analysis of reactor containment building considering severe weather condition
Y. Lee, Y.-Y. Kim, J.-H. Hyun and D.-G. Kim 152
Probabilistic assessment of a reactor pressure vessel subjected to pressurized thermal shocks by using crack distributions
G. Qian, V.F. González-Albuixech and M. Niffenegger 312
Simulation of reinforced concrete short shear wall subjected to cyclic loading
Y.M. Parulekar, G.R. Reddy, K.K. Vaze, P. Pegon and H. Wenzel 344
3D DEM simulation and analysis of void fraction distribution in a pebble bed high temperature reactor
X. Yang, N. Gui, J. Tu and S. Jiang 404

Materials Engineering
Development of recycling processes for clean rejected MOX fuel pellets
P.M. Khot, C. Singh, B.K. Shelke, B. Surendra, M.K. Yadav, A.K. Mishra, Mohd. Afzal and J.P. Panakkal 227

Material Properties
Concentration dependence of physical properties of liquid NaF–LiF–NdF_3 alloys
L. Bulavin, Yu. Plevachuk, V. Sklyarchuk, A. Omelchuk, N. Faidiuk, R. Savchuk, I. Shtablavyy, V. Vus and A. Yakymovych 60
Assessment of exposure buildup factors of some oxide dispersion strengthened steels applied in modern nuclear engineering and designs
V.P. Singh, M.E. Medhat and N.M. Badiger 90
Measurement of void fraction in flow boiling of ZnO–water nanofluids using image processing technique
K.B. Rana, G.D. Agrawal, J. Mathur and U. Puli 217

Reactor Engineering
Implementation and validation of the condensation model for containment hydrogen distribution studies
S.R. Ravva, K.N. Iyer, S.K. Gupta and A.J. Gaikwad 34
Negative power coefficient on PHWRs with CARA fuel
H.A. Lestani, H.J. González and P.C. Florido 185
Numerical investigation on practicability of reducing MCST by using grid spacer in a tight rod bundle
X. Zhu, S. Morooka and Y. Oka 198
Neutron flux monitoring system of the French GEN-IV SFR: Assessment of diverse solutions for in-vessel detector installation
C. Jammes, N. Chapoutier, P. Filliatre, J.-P. Jeannot, F. Jadot, D. Verrier, A.-C. Scholer and B. Bernardin 273

(Contents continued on back cover)

Available online at www.sciencedirect.com
ScienceDirect

Affiliated with the European Nuclear Society (ENS) and with the International Association for Structural Mechanics in Reactor Technology, e.V. (IASMiRT)

Nuclear Engineering and Design 270 (2014) 185–197

Contents lists available at ScienceDirect

Nuclear Engineering and Design

journal homepage: www.elsevier.com/locate/nucengdes

Negative power coefficient on PHWRs with CARA fuel

H.A. Lestani[a,b,*], H.J. González[c,b,d], P.C. Florido[b,1]

[a] Comisión Nacional de Energía Atómica – Centro Atómico Bariloche, Av. E. Bustillo 9500, S. C. de Bariloche, Río Negro, Argentina
[b] Instituto Balseiro – Universidad Nacional de Cuyo, Av. E. Bustillo 9500, S. C. de Bariloche, Río Negro, Argentina
[c] INVAP S.E., Av. Cmte. Luis Piedrabuena 4905, Argentina
[d] Consejo Nacional de Investigaciones Científicas y Tecnológicas, Av. Rivadavia 1917, CABA, C1033AAJ, Argentina

HIGHLIGHTS

- A PHWR fuel was optimized to obtain a negative power coefficient.
- Fuel cost, being a measure of design investment efficiency, was optimized.
- Influence on power coefficient of geometrical and economical parameters' was studied.
- Different neutronic absorbers were studied; pure absorbers can be used.
- Thermal and economical models were developed to complement neutronic assessment.

ARTICLE INFO

Article history:
Received 12 August 2013
Received in revised form
17 December 2013
Accepted 24 December 2013

ABSTRACT

A study of power coefficient of reactivity in heavy water reactors is made analyzing the reactivity components of fuels with several modifications oriented at reducing the coefficient. A cell model is used for neutronics calculations; a non-linear two dimensional model is used to evaluate the thermal changes that follow a power change; and a levelized unit energy cost model is used to assess the economical feasibility of the design changes introduced to reduce power coefficient.

The necessity of modelling all the aforementioned quantities in a coupled scheme is stressed, as a strong interdependence was found. A series of design changes complied with a negative power coefficient of reactivity, with a feasible power radial distribution and with low refuelling cost. Some investigation lines that exceed the fuel cell study and deal with the plant operation are marked as potentially addressing the stable operation of big heavy water reactors.

1. Introduction

The power coefficient (PC) is the reactivity introduced per unit of thermal power change.[2] It represents the governing feedback for all normal operation transients and a very influent feedback for many accidental transients. A negative PC value assures stability for any short period power perturbation (a few seconds of period) and relaxes the conditions under which stability is obtained for long period perturbations (a few hours of period), such as Xe induced oscillations (Bell and Glasstone, 1970a, Chapter 10).

Heavy water reactors (PHWRs) have positive coolant void coefficient (VC) and under certain operating conditions fuel burnup leads to a positive PC. That is the case for the Siemens designed pressure vessel type Atucha II nuclear power plant (NPP), which is scheduled to start operating on 2014, at nominal conditions and equilibrium burnup (CNEA, 1981), going from negative to slightly positive PC from fresh core to the steady state core burnup distribution. The pressure tube type PHWR CANDU 600 reactor designed by AECL and operating in Embalse NPP since 1983 also has a positive power coefficient and the existence of 14 liquid zones with individual closed control loops (Lepp and Frketich, 1979) assures that no decoupled sub-reactor nor sub-critical mode have an undesired power excursion (McDonnel and Green, 1978), thus stabilizing the reactor power (DOE, 1980).

VC is a key parameter on safety analysis and PC a ruling feature for operational transients. Recent studies (Ward et al., 2011) show the importance of the former by stating a 1000% power increase in 0.6 s on a postulated double ended break LOCA in Atucha II. And the latter could be the cause for some short period oscillations

* Corresponding author at: Comisión Nacional de Energía Atómica – Centro Atómico Bariloche, Av. E. Bustillo 9500, S. C. de Bariloche, Río Negro, Argentina. Tel.: +54 0294 4445100.
E-mail addresses: lestanih@cab.cnea.gov.ar (H.A. Lestani), jgonzalez@invap.com.ar (H.J. González), pcflorido@yahoo.com (P.C. Florido).

[1] Private consultant.

[2] Deeper definitions and discussions are presented later in this work.

0029-5493/$ – see front matter © 2014 Elsevier B.V. All rights reserved.
http://dx.doi.org/10.1016/j.nucengdes.2013.12.056

Table 1
Atucha II core data used in the calculations.

Thermal power	2160 MW
Thermal power to moderator	220 MW
Core active length	530 cm
Equivalent core radius	303 cm
Number of coolant channels	451
Channel radius	5.418 cm
Coolant flow rate	10,300 kg/s
Coolant flow through channels	96%
Coolant inlet temperature	278 °C
Fuel element peaking factor	1.116
Coolant outlet pressure	108 MPa

(not related to Xe oscillations) that state of the art calculations (Mazzantini et al., 2011) anticipate for Atucha II.

Studies have been made since the early 70s in the sake of passive safety features for PHWR (Kay, 1976). These studies commenced in Canada, where the PHWR technology was more strongly commercially developed with the CANDU reactors, and were spread out to other countries where PHWR technology is present either as pressure tube type (CANDU) or as pressure vessel type (as is today the solely case of Argentina, with the Siemens designed PHWRs). Recently a new analysis was published on the improvement of PC for CANDU reactors in KOREA (Gyuhong et al., 2011), which indicates the interest on this topic in the aforementioned countries.

In this work a through out study of PC is made and a new approach is presented for the analysis of the physics involved and the technological solutions proposed taking the pressure vessel type PHWR Atucha II operating conditions as the base case. The thermal-hydraulics and neutronics models are implemented in accordance with verificated and validated models. The PC is calculated for a wide range of parameters combined in a large number of configurations and the fuel cycle cost per kWh is optimized for every PC and power peaking factor (PPF) value. The work aims to provide CARA, an alternative fuel design, a negative PC without higher linear power rating and fuel cost than the original Atucha II fuel.

The Atucha II core has been chosen as the base case because its operating conditions are the most demanding in terms of safety and operation compared to Embalse or Atucha I. Regarding to safety, the void coefficient in Atucha II is the biggest due to its larger core (Lestani et al., 2011a), and the fact that the two loops of the primary circuit are connected via the inlet and outlet plenums, as opposed to the CANDU design which has a splitted primary circuit (CNEA, 1979), imposes that the reactivity introduced on Large-LOCA sets the reactor as supercritical prompt. With respect to operation, besides the aforementioned aspect on VC that also affects PC, the lack of fast response systems to measure and modify core power distributions imposes restrictions on the allowed PC (Bell and Glasstone, 1970b, Chapter 9), as will be further explained.

In Table 1 the Atucha II core data used in the calculations is shown, extracted from reference (CNEA, 1981). The "Thermal Power to Moderator" item in the table refers to the thermal power transferred from the coolant to the moderator, which does not increase coolant enthalpy and has to be subtracted from the total thermal power produced in the fuel. This total "Thermal Power" is however taken into account for subcooled boiling as explained in Section 2.1. The primary circuit flow rate is divided using a small fraction (4%) to cool the moderator down, bypassing the coolant channel. The system pressure is defined by the pressurizer's pressure range at the RPV outlet, and the lowest pressure has been used in the calculations because it represents the most unfavourable condition for PC.

With 2 PHWR NPP in operation in Argentina, and a third one to start soon, each NPP requires its specific fuel, which are locally manufactured by an Argentinean company. CARA fuel design was proposed to use the same fuel bundle in the 3 different NPPs (Brasnarof et al., 2005a). A picture of CARA fuel is presented in Fig. 1. A detailed description of its mechanical and thermal-hydraulic design fundamentals can be found on the references. However, a short description of its innovations is given in the next paragraph.

Fig. 1. CARA fuel.

CARA fuel is 997 cm long, which implies that half the fuels are needed to cover the full length of a CANDU reactor, only 6. This reduction in the number of fuels and consequently, the number of endplates, allows to increase the number of rods from 37 (conventional to all PHWR nowadays) to 52, which produces an increase in the hydraulic pressure loss that could not be affordable with twice the endplates. The higher number of rods lowers the surface power density, and a higher power peaking factor is allowed, which in turn allows the use of stronger absorber materials: slightly enriched uranium (SEU) and burnable neutronic absorbers can be used. From the mechanical point of view, a collapsible cladding (no gap) of 0.54 cm is used, whose influence on the PC is studied. For vertical channel PHWRs, such as the Atucha reactors, an additional basket was designed (Brasnarof et al., 2005b). More geometrical specifications and reference values for the neutronic parameters will be given in Tables 6 and 7.

2. Calculation methods and models

A thermal power change will lead to gap thickness, density, temperature and thermal conductivity changes in the fuel rod, temperature and density (void fraction) changes in the coolant and moderator, expansions (and perhaps asymmetrical deformations) in structural materials. These changes imply a reactivity change. For the PC, the thermal power change itself has no direct effect on reactivity,[3] but it has the indirect short term effects (a few seconds) mentioned above that do introduce reactivity, and also mid term effects (a few hours) that affect reactivity (as the saturable poisons concentrations).

A thermal model is then mandatory to *translate* the postulated perturbation into the corresponding parameters that affect neutronics.[4] Then the question arises of what effects have to be included in the thermal model. Looking for short term stability, i.e., for rapid feedback that would be desirable to be self-controlled without the actuation of any control system (Bell and Glasstone, 1970b, Chapter 9), the saturable poisons concentrations are excluded, considering that these concentrations change with periods of hours. Besides, no asymmetric deformation nor

[3] The neutron transport equations are not affected by an increase (or decrease) in the neutron flux, provided the spectrum remains unaltered and neglecting fission products poisoning.

[4] Strictly speaking, the model might include thermal, hydraulic, mechanical and burnup phenomena.

axial bending has to be expected.[5] Such is the thermal model used in this work.

2.1. Thermal model

A thermal model including non-linear heat conduction in the pellet, pellet–cladding physics and heat removal by the coolant subject to subcooled boiling was implemented. The bulk coolant temperature axial profile ($T(z)$) is obtained by integrating the heat flux in the axial direction:

$$\dot{m}Cp_{D_2O}\frac{\partial T_{D_2O}}{\partial z} = q\prime(z)$$

where $\dot{m}$ is the coolant mass flow, T_{D_2O} is the mean coolant temperature and q' is the linear heat flux. $\dot{m}$ and q' have to be consistently defined as either channel or sub-channel values. The proper dependence of the parameters on temperature (Cp_{D_2O}, Enthalpy, Density) is modelled by the use of tabulations. At this stage thermodynamic equilibrium conditions are obtained but special considerations have to be made for subcooled boiling, which occurs for extensive regions of the core at operating conditions (CNEA, 1981). To cope with that the *void drift model* for subcooled boiling developed with the Levy profile (Todreas and Kazimi, 1993) has been used:

$$Void(z) = \frac{1}{C_0(1+((1-x(z))/x(z))(\rho_g/\rho_l))+(V_{gj}/x(z)G)\rho_g} \quad (1)$$

where $Void(z)$ is the void fraction, ρ_g and ρ_l are the steam and liquid densities, respectively, G is the mass flow per unit area, $x(z) = x_e(z) - x_e(z_d)e^{(x_e(z)/x_e(z_d))-1}$ is the Levy flow quality with x_e being the equilibrium thermodynamic quality and z_d the point of bubbles departure. A detailed explanation of the Saha and Zuber correlation for z_d and of the coefficients C_0 and V_{gj} that depend on the liquid and flow properties can be found on reference (Todreas and Kazimi, 1993). An iterative scheme has to be implemented due to the mutual dependence of the void fraction ($Void$) and the liquid enthalpy.

The heat transfer between cladding and coolant is modelled with the Dittus–Boelter correlation ($h_{DittusBoelter}$) in the one-phase points of the channel and the Chen correlation (Todreas and Kazimi, 1993) is used where subcooled boiling is present:

$$h_{SubcooledBoiling} = h_{DittusBoelter} + h_{Forster-Zuber}$$

i.e., a new term ($h_{Forster-Zuber}$) is added to the Dittus–Boelter transfer coefficient to account for the enhanced convection when boiling is present.[6] This correction to the heat transfer coefficient requires an iterative calculation, as the cladding temperature and the $h_{Forster_Zuber}$ depend on each other. The cladding temperature is obtained as a result, which imposes the border condition for the thermal transfer in the pellet–clad system.

The fuel pellet temperature profile in 2-D cylindrical (r, z) geometry was obtained by solving the 1-D radial heat transfer equation with the linear power density (q') and pellet border temperature (T_s) corresponding to each axial position (z)[7]:

$$\frac{1}{r}\frac{\partial}{\partial r}\left(rK_{UO_2}\frac{\partial T}{\partial r}\right) + q''' = \rho_{UO_2}Cp_{UO_2}\frac{\partial T}{\partial t}$$

where K_{UO_2} is the conductivity of the fuel, that depends on T, the fuel temperature at that point, and q''' is the volumetric heat source. ρ_{UO_2} and Cp_{UO_2} are the density and the specific heat of the fuel, respectively. The integration of this equation yields to the well-known result that the linear heat density (which is considered radially constant) in the annular section limited by (r_c, r_s) is related to the conductivity integral by the following equation:

$$\int_{Ts}^{T_c} K\,dT = q'''\frac{r^2}{4}\Big|_{r_c}^{r_s} = \frac{q'_{r_s-r_c}}{4\pi}$$

Hence, the use of a fitted thermal conductivity integral allows to obtain the temperature radial profile accounting for non-linearities in the fuel conductance.

Conductance through the gap requires coupled thermo-mechanical calculations due to the high sensibility of the temperature jump in the gap thickness and vice versa. In this work a model for beginning of life[8] was implemented, including thermal expansion, mechanical deformation (due to coolant external pressure or when pellet–cladding contact occurs), and specific models for conduction in the Knudsen domain.[9] The Ross & Stoute model (Tong and Weisman, 1996) was used for the gap thermal conductance when pellet–cladding contact occurs and the McDonald and Weisman model (Tong and Weisman, 1996) for cracked pellets when the gap thickness is not zero. Analytical theory of elasticity (Budynas-Nisbett, 2006) was used to estimate the mechanical deformation and contact pressure. The UO_2 and Zr_4 properties were taken from the reference (Hagrman and Reymann, 1979).

All these equations allow to obtain the aforementioned temperature and density profiles, with which adequate channel mean values can be taken. To estimate the temperatures evolution in a power transient, these channel averaged values were used in a Lumped Parameter Model (Lewis, 1977) described by the equations:

$$M_{fuel}Cp_{fuel}\frac{dT_{fuel}}{dt} = P(t) - P_{conv}(t)$$

$$M_{cool}Cp_{cool}\frac{dT_{cool}}{dt} = P_{conv}(t) - P_{cool}(t)$$

$$P_{conv}(t) = \frac{T_{fuel}(t) - T_{cool}(t)}{R_{rod}}$$

$$P_{cool} = 2\dot{m_{cool}}Cp_{cool}[T_{cool}(t) - T^{in}_{cool}(t)]$$

where the subscript *fuel* stands for the pellet and clad weighted properties and *cool* corresponds to the coolant, the superscript *in* refers to properties at the channel inlet, M is the fuel element mass, P is the thermal power, R_{rod} is the fuel, gap, cladding and convective thermal resistance.

In this manner a simple Lumped Parameter Model is able to account for non-linearities in pellet heat conduction, gap thickness and water properties. It has to be mentioned that the time modelling corresponds to the so-called "quasi-static approximation", since the spatial profiles correspond to the steady state in each instant.

2.2. Neutronic cell model

The neutron physics cell code WIMSD-5 was used with the WLUP 69 groups library (IAEA, 2013) to calculate the reactivities

[5] One should bear in mind, however, that misregarded mechanical deformations seemed to be responsible for erroneous estimation of the PC in the MAPLE reactors (Parliament of Canada, 2009).

[6] Furthermore, the Dittus–Boelter term is applied a correction factor to account for bubbles existence, as can be seen on the detailed explanation of reference (Todreas and Kazimi, 1993).

[7] This approach assumes no heat transfer in the axial direction, which is based on the fact that the radial thermal gradient is a few hundreds of times greater than the axial thermal gradient, and so is the relation between the fluxes.

[8] Irradiation effects were not taken into account: fission gas release, composition change, swelling, pore migration, etc.

[9] Conduction through a gas gap thinner than the gas molecules mean free path.

introduced by the temperature and density changes caused by a power perturbation, i.e., to calculate de PC. The TEMPERATURE and DENSITY options of the code input file were used to introduce perturbations at each burnup level during infinitesimal burnup steps (IBS). An IBS is a step so small as to produce no significant change on the composition, but its existence is sufficient to use the code for a new estimation of the multiplication factor (K), including perhaps a modification on any temperature or any parameter of the calculation. A brief discussion is needed to clarify this procedure and to avoid misinterpretations induced by the code scheme.

The output file of WIMSD-5 contains (amongst many other data) sets of burnup levels and the corresponding K's, each one calculated for the composition of the previous burnup step. As a consequence, if an IBS with no perturbation is made after a finite burnup step, a finite K change ($\Delta K = K_2 - K_1$) will be observed due to the previous composition change (and not related to the present negligible composition modification). To obtain a negligible ΔK at least two IBS should be performed, giving as a result an unperturbed K, after which an IBS with a modified parameter could be performed obtaining the perturbed K, their difference being the ΔK due to the parameter modification. For numerical reasons even after two IBS with no perturbation a small ΔK is obtained, and this fact imposes a limit to the minimum perturbation observable. A set of comparisons with explicit perturbations (not using IBS but making different runs for the reference and perturbed states) served as verification and allowed to set proper limits to the minimum perturbations that could be made.

With this procedure the PC was obtained as a function of burnup. Two quantities of high relevance are also obtained from the neutronic model, namely, the power peaking factor (PPF) and the average extraction burnup of the fuel element (B_{ext}). The maximum PPF during the whole in-core life of the fuel element is taken as the representative value. The fuel element life or B_{ext} is assessed by the integral method, i.e., the limit for continuous refuelling of the Non-Linear Reactivity Model (Driscoll et al., 1990). In this approach, B_{ext} is the burnup level at which the area of $K(B)$ over $K = K_w$ is equal to the negative area of $K(B)$ below $K = K_w$:

$$\int_{B=0}^{B_{ext}} (K - K_w)dB = 0 \tag{2}$$

where B is the burnup level and K_w is the working K and defines a desired reactivity excess. This method is appropriate for continuous refuelling reactors (Driscoll et al., 1990).

The value of PC taken as representative for the design modifications was also the maximum at all burnup levels. Hence, a negative value would imply that no region in the core will have positive feedback, avoiding the rapid power excursions that might occur in large reactors without local power control.[10]

2.3. Fuel cycle cost model

A fuel cycle cost model was implemented to cope with the necessity of having a proper figure of merit to assess the viability and to measure the benefits of design changes. A simpler approach would be the use of B_{ext} as such figure of merit, considering that it measures the energy that can be extracted from the fuel. However, it would lack information about how much investment is required to obtain that fuel and therefore, that energy. Optimization of B_{ext} imposes no limit on the enrichment (ϵ), as it is a monotonically rising function of ϵ. The fuel cost per unit energy, however, being the ratio of investment to energy extracted has an optimum ϵ value, representing the competition between the B_{ext} and investment rises with ϵ.

In this work a very simple model of levelized unit fuel cost (*LUFC*) was calculated as explained in the IAEA Manual on Economics (IAEA, 2008). *LUFC* is basically the ratio of fuel cost to the energy it produces. The costs and the energy produced are levelized in time using a discount rate d. The costs include only those related to fabrication of new fuels according to the refuelling strategy. Amortization of first core was not included in the analysis because the cores of the argentinian reactors already exist, and any design modification to this new fuel element will not change the cost implied in the amortization of the already invested core. It was also assumed that no change in the operation and maintenance costs of the plant will occur as a consequence of design modifications to the fuel. Therefore, *LUFC* only accounts for refuelling costs.

$$LUFC = \frac{\$^{Fuel}_{Investment}}{Energy\ Produced}$$

For the evaluation of the above equation the values presented in Table 2 were used. The calculated costs were used as a comparative figure of merit among different designs. Effort has been put on the accuracy and consistency of the economic model. However, some of the values presented in the table, taken from international references, might not be directly applicable to the small argentinian market. Furthermore, the use of a SWU (Separative Working Units) model for the enrichment cost might be replaced for a simpler linear cost model, according to down-blending of commercial enriched uranium (considering that SEU is obtained from down-blending in Argentina). However, any attempt to have a more precise definition of these variables would imply the knowledge of political decisions which are far beyond the scope of this work. The refuelling cost, despite the possibility of being outdated or subject to commercial conditions of doubtful application to Argentina, has much more information than the exclusively neutronic criteria and its uncertainty reflects a true fact on nuclear policies.

Table 2
Data used in the cost calculations.

Core data	
U inventory	88.74 tn
Refuelling zones	451 (continuum)
Load factor	95%
Thermal efficiency	35%
Cost data	
Item	Cost (time required)
U_3O_8	70 US$/kgU (2.5 years)
UF_6 conversion	8 US$/kgU (2 years)
Enrichment	140 US$/SWU (1.5 years)
UO_2 conversion	8 US$/kgU (1 year)
Cladding – assembling	250 US$/kgU (1.5 years)
Discount rate	8%
First core amortization	30 years

2.4. Verification and validation

A series of long lasting verification and validation (V&V) calculations were performed to assess the uncertainty of the models implemented. The results compared include some isolated models, i.e., neutronic or thermal, as a first step. Whole model results involving neutronic-thermal feedback were assessed as a further step.

2.4.1. Neutronic V&V

The uncertainty for two neutronic quantities of great importance for PC, as explained in Section 3, were assessed. Void coefficient, the first quantity of interest, was validated against an experimental benchmark of the DCA reactor (KAERI, 2001) and a

[10] The reactor at Point Lepreau experienced a sharp power excursion activating both shutdown systems due to malfunction in one of the fourteen Liquid Zone Control Systems (CNSC, 2007).

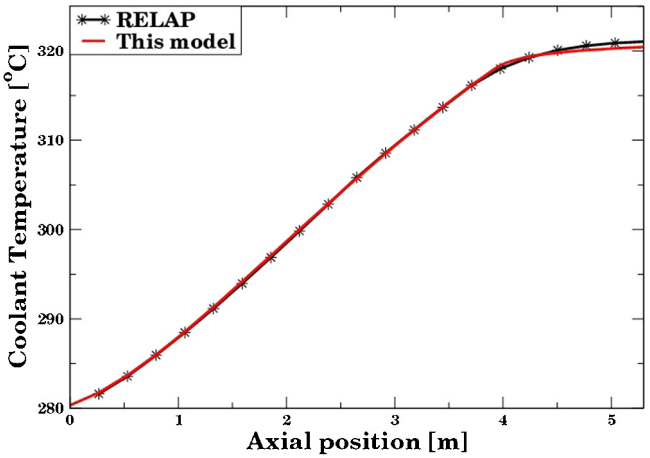

Fig. 2. Verification of the temperature axial profile against RELAP 5.

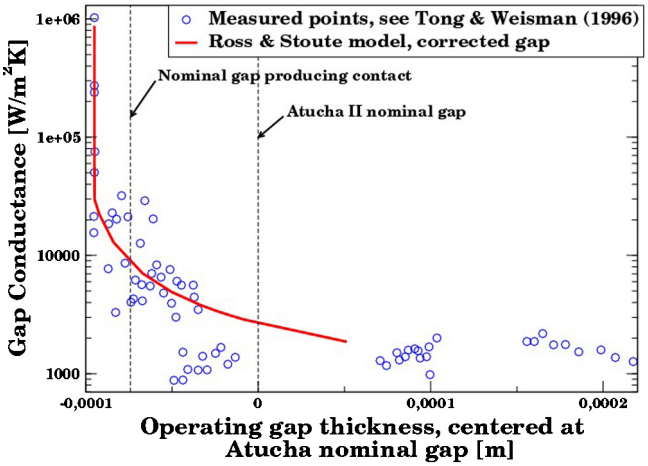

Fig. 4. Gap conductance as a function of gap thickness.

prediction uncertainty defined by a standard deviation of 150 pcm was obtained, as can be seen on reference (Lestani et al., 2011a). The uncertainty on the fuel temperature coefficient of reactivity, the second quantity of interest, was verificated against a numerical benchmark (Rahnema and Gheorghiu, 1996) and a numeric uncertainty defined by a 26% mean bias was obtained, as can be seen on reference (Lestani et al., 2011b). This represents a strong source of uncertainty. The difference in the manner the uncertainties were assessed is a consequence of the type of benchmark run and the number of cases studied for each quantity.

2.4.2. Thermal verification

The thermal model underwent two numerical verifications involving the most important quantities. As a first step the axial profiles of the coolant properties were compared against the results from a RELAP 5 (ISS, 2013) sub-channel model. In Figs. 2 and 3 the comparisons for coolant temperature and coolant void are shown for an average channel. The power ranges up to 170%, far beyond the maximum power allowed for the reactor, and was chosen solely for the comparison in order to achieve high void fractions and study the differences between the model and the RELAP results.

It can be seen in Fig. 2 that both estimations of coolant temperature agree very well before subcooled boiling begins at about 3.7 m, the difference being less than 0.2 °C. A bigger difference is observed, however, beyond that position, reaching up to 0.6 °C at channel outlet. This is due to a difference in the void fraction prediction and hence a difference in the phase change enthalpy subtracted from the liquid enthalpy. The origin of the void fraction differences is that RELAP 5 uses a different correlation than the one used here and presented in Eq. (1). The correlation used in this model gives lower void fractions at channel outlet for low power (up to 125%) but higher void fractions at channel outlet for high power (>125%), as can be seen in Fig. 3.

The second thermal quantity of high sensitivity that was subject to verification is the pellet–cladding gap thermal conductance. In Fig. 4 some measured conductances (Tong and Weisman, 1996) are shown and a huge dispersion can be observed, reaching up to one order of magnitude at about -5×10^{-5} m. The Ross and Stoute model (Tong and Weisman, 1996), shown with a continuous line, was used in this work calculated with a gap thickness corrected to account for thermal expansion of pellet and cladding, and for mechanical compression of the cladding (due to coolant pressure). It has to be noticed that measurements were reported for operating gap thickness, not for nominal dimensions.

The thermal conductance is such a sensible parameter that thermal and mechanical expansion corrections to the gap thickness lead to 70 °C of temperature decrease at pellet border, 120 °C decrease at pellet centre and 97 °C decrease in the mean pellet temperature, according to this model. For this reason a big effort was put to predict the gap thickness corrections, which were calculated in accordance with the models implemented in the BaCo code (Marino, 2011).

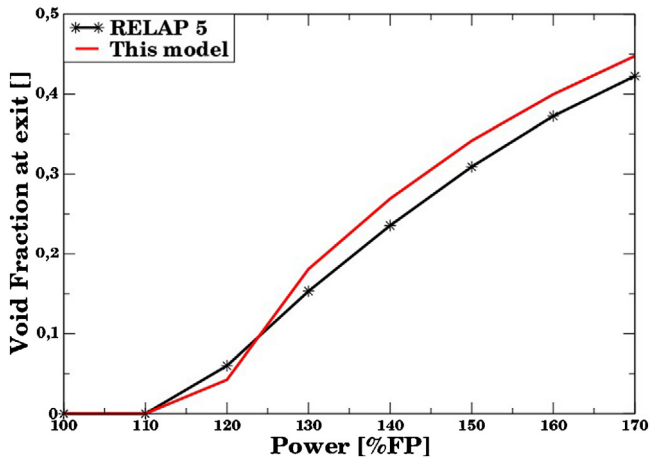

Fig. 3. Verification of the void fraction at channel outlet against RELAP 5.

2.4.3. Power coefficient coupled verification

A comparison of the results of the thermal and neutronic coupled calculations involved in the power coefficient was made with the data presented in the preliminary safety analysis report (PSAR) of the Atucha II NPP (CNEA, 1981). The comparison is summarized in Table 3, where 4 different reactivity coefficients are shown.

It can be seen that the power coefficient predictions agree very well with those reported in the PSAR, the biggest bias corresponding to the equilibrium burnup state, where all the uncertainty of the isotopes evolution adds to the uncertainty of the intrinsic modelling of the power coefficient. It can also be seen, as stated in Section 2.4.1, that the FTC poses an important source of uncertainty.

A column with the values at end of life (EOF) burnup was added in Table 3 to give an idea of the range of values in the core. The refuelling strategy of Atucha II divides the core in four radial zones, numbered 1–4 from the centre outwards. The freshest fuels are located in zones 3 and 2, while the oldest fuels are located in zones 4 and 1. This commonly used refuelling strategy, as opposed to a

Table 3
Comparison of reactivity coefficients with the PSAR values.

	BOL[a] 0 ppm boron		BOL 7 ppm boron		BEQ[b] 0 ppm boron		EOL[d] 0 ppm boron	
	PSAR	Model	PSAR	Model	PSAR	Model	PSAR	Model
Fuel temperature coefficient [pcm/°C]	−1.0	−1.28	−1.1	−1.42	−0.3	−0.18	–	0.16
Coolant temperature coefficient[c] [pcm/°C]	3.2	2.59	3.7	3.36	7.4	5.31	–	6.9
Coolant void coefficient [pcm/%void]	14	13.5	16	17	11	12	–	12.75
Power coefficient [pcm/%FP]	−4.4	−4.49	−4.6	−4.77	0.3	0.87	–	2.9

[a] *BOL* refers to beginning of life with ^{135}Xe and ^{149}Sm equilibrium concentrations.
[b] *BEQ* refers to equilibrium burnup, defined in PSAR as 4000 MWd/tonU.
[c] PSAR defines CTC including the effect of density changes.
[d] *EOL* refers to end of life. No values reported in the PSAR.

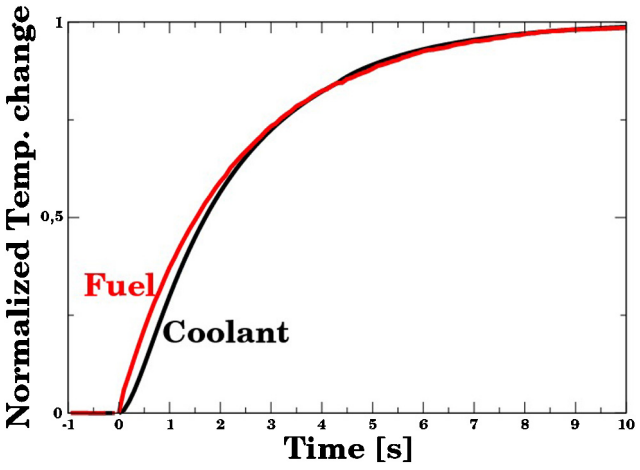

Fig. 5. Normalized temperatures evolution on a power increase. Negligible delay is observed in coolant heating with respect to fuel.

"scattered core" strategy,[11] groups the fuels with similar burnup levels into zones where the local stability is governed by the PC at a zone-equivalent burnup. As a result, the fuels with the higher positive PC are grouped together posing a threat to local stability, even if weight averaged coefficients for the whole core suggest global stability. This difference between local and global stability explains why reactors with 'near zero' global power coefficient of reactivity needed to implement zonal reactivity control, as the two PHWR developments at AECL in Canada (McDonnel and Green, 1978) and at NPCIL in India (NPCIL, 1995).

3. Power coefficient physics

According to the implemented model, the coolant temperature increase as a consequence of a power rise is negligibly delayed with respect to the fuel temperature increment, as can be seen in the normalized temperature plot of Fig. 5. Normalization was made according to:

$$T^i_{norm} = \frac{T^i_{(t)} - T^i_{(t=0)}}{T^i_{(t=\infty)} - T^i_{(t=0)}}$$

where T_{norm} refers to the normalized temperature, the superscript i can be "fuel" or "coolant", $T_{(t=0)}$ is the temperature before the transient and $T_{(t=\infty)}$ is the stationary temperature after the transient.

This result implies that, assuming a linear dependence of reactivity within the perturbation range, the reactivity introduced during a power transient will have the same shape as that of Fig. 5. In this work the calculated PC corresponds to the final state of the transient and any previous instant will therefore have a smaller reactivity insertion. The consideration of non-linearities would make small deviations on the shape of the reactivity introduced, but not on its steady state value, for which fuel and coolant non-linearities are explicitly modelled as described in Section 2.1.

3.1. PC decomposition

The study of *PC* physics was made observing each reactivity component, according to the following decomposition:

$$PC = \frac{d\rho}{dP} = \frac{d\rho}{dT_{fuel}}\frac{dT_{fuel}}{dP} + \frac{d\rho}{dT_{cool}}\frac{dT_{cool}}{dP} + \frac{d\rho}{dVoid}\frac{dVoid}{dP} \quad (3)$$

where $\rho = ((K-1)/K)$ is the reactivity, P is the thermal power and *Void* is the flat weighted along the channel void fraction $Void(z)$, obtained from Eq. (1). The derivatives $(d\rho/dT_{fuel}) = \alpha_{fuel}$, $(d\rho/dT_{cool}) = \alpha_{T_{cool}}$ and $(d\rho/dVoid) = \alpha_{void}$ are the fuel temperature, the coolant temperature and the coolant void coefficients of reactivity. $\alpha_{T_{cool}}$ normally accounts for coolant density changes also, but this effect was presented explicitly due to its relevance.

The reactivity contribution from the coolant temperature ($\alpha_{T_{cool}}$) is small compared to the other two terms, as could be expected in a HWR. In this work the effort was focused on the fuel temperature (α_{fuel}) and the coolant void (α_{void}) contributions to reactivity. Measures that can be implemented to make these terms smaller or negative are studied in the following paragraphs.

3.2. Void coefficient

The reactivity introduced on coolant voiding increases linearly with the void fraction as shown in Fig. 6. For this reason, the small coolant density decrease caused by a power rise introduces a proportional fraction of the coolant void reactivity corresponding to 100% void (*CVR*). A *PC* reduction is thus achieved in the 3rd term of Eq. (3) by reducing the *CVR*.

The *CVR* was deeply studied for many years and a previous work applied to the CARA geometry can be found on reference (Lestani et al., 2011a). Some conclusions from that work are of interest for the present study and can be summarized as follows.

- A K_∞ radial distribution is needed in the bundle in order to introduce negative reactivity on coolant voiding due to flux flattening produced in the fuel bundle. i.e., $K_\infty^{Innerrods}$ has to be smaller than $K_{\inf}^{Outerrods}$. This gradient is produced with the use of burnable neutronic absorbers (BNA) in the inner rods and the use of slightly enriched uranium (SEU) in the outer rods.
- The BNA can be introduced co-sintered in the UO_2 pellet or in pure absorber oxide rods, with better costs and less technological difficulties in the latter. Thermal absorbers are preferred rather than those with big epithermal resonances, and the burnup rate should be balanced to assure appreciable effect but to last up to

[11] A scattered core refuelling strategy is that in which the burnup level is uniformly distributed across the core.

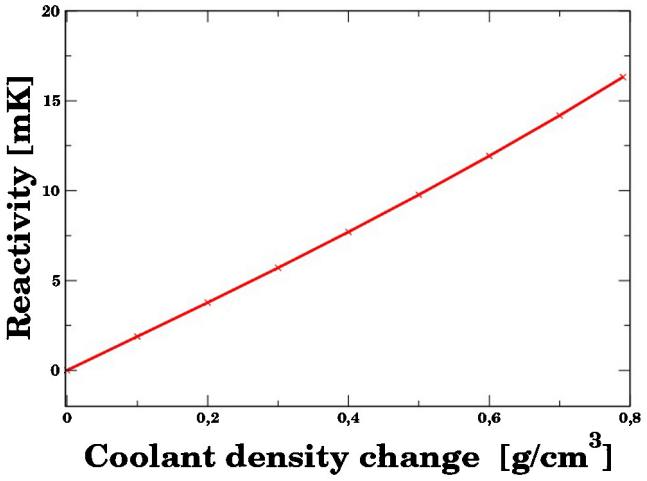

Fig. 6. Linearity of coolant void reactivity according to the WIMSD-5 model.

mid-burnup. Dy_2O_3, In_2O3 and B_4C proved to give satisfactory results when looking for negative VC.

- The ^{235}U enrichment has to be risen to counterbalance the burnup fall due to the absorbers. The proper enrichment level is found on cost requirements.
- The enrichment distribution should avoid steep power peaking. Optimum distributions were found to cope with this objective.
- A few different fuel configurations can satisfy the negative *CVR*, low cost and low PPF objectives pursued.

Other measures to reduce the positive reactivity introduced by steam bubbles represented by the 3rd term of Eq. (3) have been analyzed. These measures range from rising the pressurizer's lower pressure setpoint to flattening the axial power distribution. The effect of the pressure on the coolant void fraction is shown in Fig. 7. It can be seen that a pressure increase drastically lowers the bubbles formation, hence a reduction on the 2nd factor of the 3rd term of Eq. (3) is obtained. Similarly, if the power density is lowered near the channel outlet, where subcooling is poor and the conditions for subcooled boiling are present, the void fraction decreases.

To keep the scope of this work within fuel bundle modifications, these reactor modifications aiming at reducing bubbles generation will not be further studied here.

It must be noticed, however, that besides any *CVR* reduction achieved by the measures previously enumerated, the 3rd term is reduced by the simple fact that CARA fuel has less surface heat flux (for having 52 rods instead of 37), producing less subcooled boiling at the same operating conditions and hence introducing less positive reactivity on a power increase.

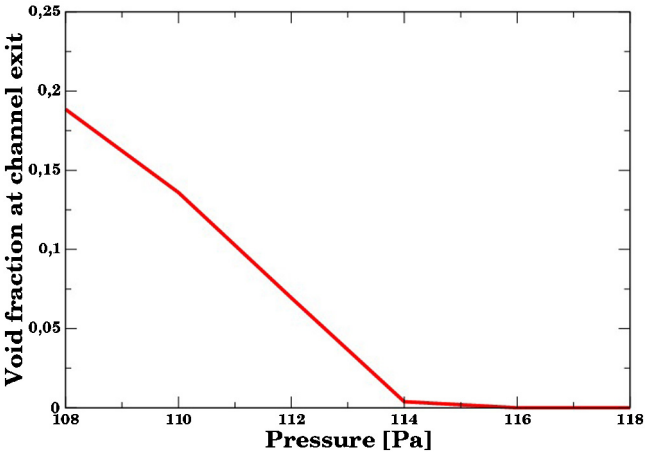

Fig. 7. Void fraction at channel exit for different operating outlet pressures, at 110% of full power.

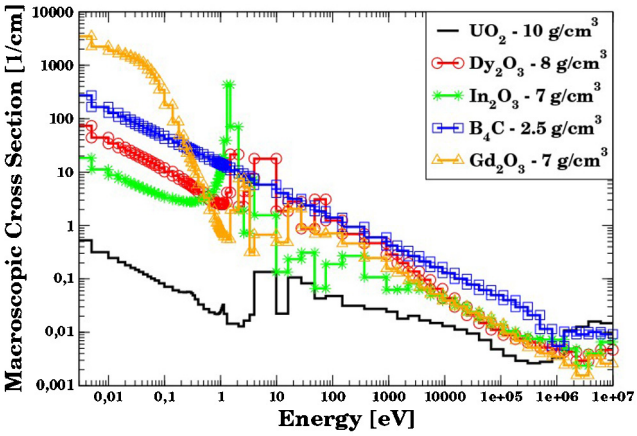

Fig. 8. Cross sections resonances for different BNAs.

3.3. Fuel temperature coefficient

The fuel temperature coefficient (FTC) is the reactivity introduced per Celsius Degree (°C) of heating of the fuel pellet. The main cause for this reactivity is the Doppler broadening of the resonances. The sign of this contribution depends upon the relative weight of capture and fission resonances, and how they compete and weight. As a general rule, the presence of ^{239}Pu moves the FTC towards positive values as a consequence of its large fission resonances.

Another effect, usually not mentioned, not related to Doppler broadening composes the FTC and gains importance when ^{239}Pu is present. It is the spectral shift of thermal neutrons which are upscatterd in the oxygen atoms, as was measured by Time of Flight (Johansson, 1987). This spectral shift produces a flux increase in the vicinity of the 0.3 eV ^{239}Pu resonance, and thus introduces positive reactivity.

It is observed in Table 3 and more precisely in Fig. 14 that the FTC is negative for beginning of life (BOL) and moves towards positive values with the ^{239}Pu buildup, achieving positive values near the end of life (EOL). This is confirmed by state of the art calculations of the FTC (Yonghee, 2012). It is therefore desirable to reduce the buildup of ^{239}Pu, provided once built, no modification can be thought of that affects only ^{239}Pu resonances and not ^{238}U resonances, which introduce a net negative reactivity.

3.3.1. Burnable neutronic absorbers

The effects of BNAs in the ^{239}Pu buildup and its positive FTC were studied. Four different absorbers were studied: Dy_2O_3, In_2O_3, B_4C and Gd_2O_3, and the effects found were classified into three categories:

(a) *A reduction in ^{239}Pu production.* This reduction is a consequence of the shielding of the capture resonances of ^{238}U due to higher absorption in the epithermal range when BNAs are used, as can be seen on the cross sections plot of Fig. 8. The ^{239}Pu evolution for different BNA compositions can be seen in Fig. 9, where correlation can be made of how much ^{239}Pu reduction is observed and how much epithermal absorption adds the BNA. With this criterion, when the same BNA percentage is used, the preferred BNA rank is B, Dy, Gd and In.

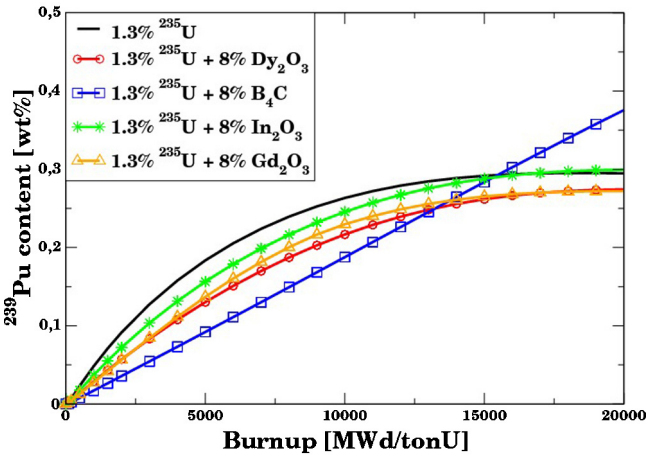

Fig. 9. ^{239}Pu build up for different BNAs.

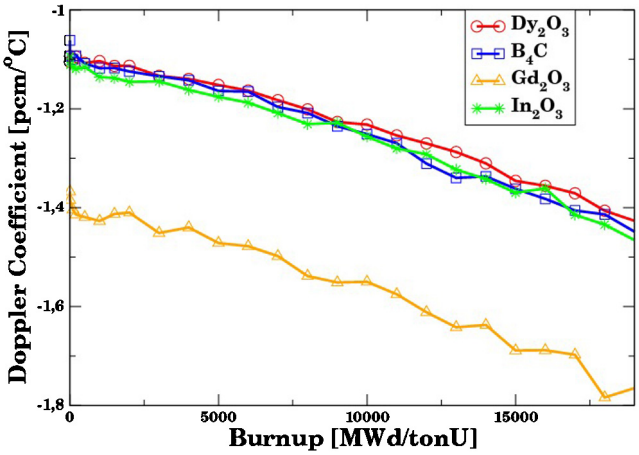

Fig. 10. Negative reactivity from Doppler broadening of the BNAs resonances.

However, if equivalent compositions are used[12] instead of equal percentages, the result obtained is qualitatively similar to that of Fig. 9 but with the following BNA rank: Gd, B, Dy and In. These comparisons were made observing the reduction on the ^{239}Pu production rate at low burnup, which varies as the BNA gets burnt and the ^{239}Pu concentration tends to an equilibrium value given by the equation:

$$N_{239Pu(t\to\infty)} = N_{238U(t\to\infty)} \frac{\int_0^\infty \Phi(E)\sigma_c^{238}\,dE}{\int_0^\infty \Phi(E)\sigma_a^{239}\,dE} \quad (4)$$

Interpreting the cross sections in the above equation as weighting functions for the fluxes and knowing that the strongest ^{239}Pu absorptions are thermal and that the strongest ^{238}U captures are epithermal, the fraction in the previous equation is a measure of the spectrum hardening. The spectrum hardening produced by the different BNAs and their daughters explains why the final ^{239}Pu concentrations in Fig. 9 are different.

(b) *The addition of resonances.* Most absorbers have strong resonances and they introduce negative reactivity when they undergo heating. The reactivities shown in Fig. 10 were obtained rising the temperature of two central rods in the fuel having a ceramic of the named absorber without fissile material. Such reactivities are plotted against burnup, and they last up to high burnup thanks to the onion skin effect (Knott and Yamamoto, 2010) and the build up of the BNAs daughters. The biggest negative reactivity due to Doppler broadening is obtained with Gd, followed by In, B and Dy. It might be concluded that the stronger the resonances and the lower their energies (getting away from the energies shielded by ^{238}U resonances), the stronger the negative Doppler reactivity.

In order to make use of this potential negative reactivity, the BNAs should be mixed with the UO_2. Otherwise the BNAs will not be properly heated in a power transient, considering that the coolant temperature jump is much smaller than the fuel temperature jump, and this negative reactivity feature might not be fully used.

(c) *Shading of ^{238}U resonances broadening.* The Doppler-caused increase on effective cross sections is shaded by the presence of absorbers, as shown in Fig. 11. To obtain the values of the ordinate axis of Fig. 11, the fuel containing the BNA was heated up, and the cross section increase obtained at each energy group was normalized to the group cross section. The graph shows results for equivalent compositions of different absorbers. Analyzing the reduction of absorption increase by Doppler effect due to the presence of other absorbers and their absorption cross sections, shown in Fig. 11, and the cross sections of Fig. 12, the following observation can be made. The higher the BNA resonances energies the stronger the reduction, considering that most of the used BNAs have resonances at lower energies than

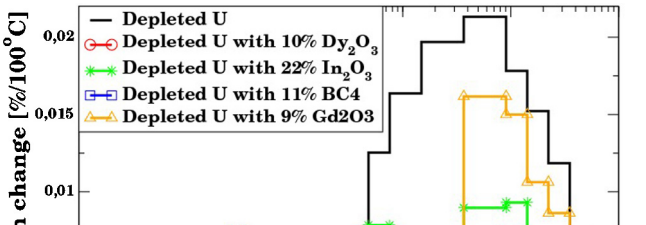

Fig. 11. Weight reduction in Doppler broadening of U resonances due to the presence of BNA.

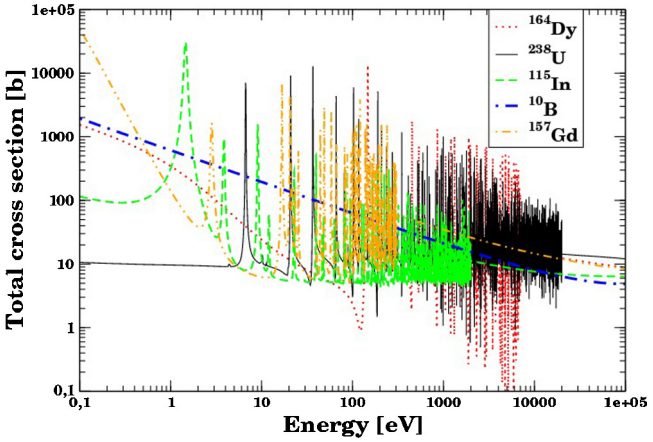

Fig. 12. BNAs cross sections.

[12] Those compositions having similar effects on void coefficient at low burnup are considered as equivalent.

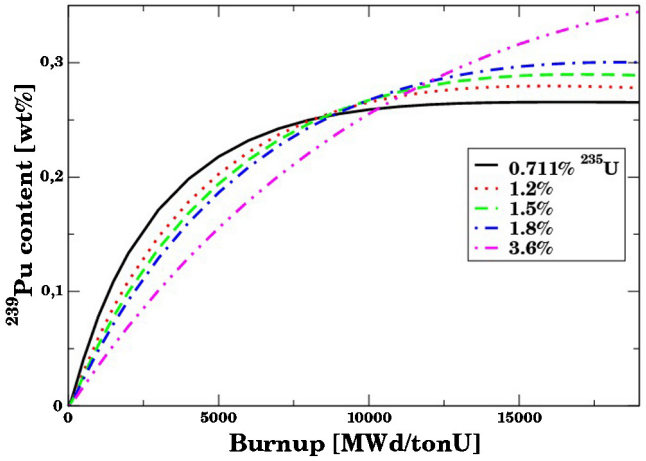

Fig. 13. ^{239}Pu build up for different enrichment grades.

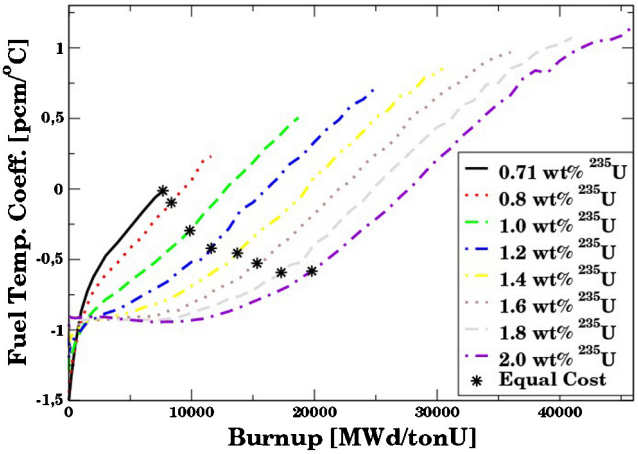

Fig. 14. FTC evolution with burnup for different enrichment grades.

they are in ^{238}U (reaching up to 20 keV and leaving an energy band without interfering with ^{238}U resonances). With this criterion the BNAs that reduce the most the absorption increase due to Doppler effect on ^{238}U are the following, in increasing order: Gd, In, B, Dy.

All these effects combined determine the FTC and its dependence with burnup. Fuel design modifications directly affect BNA amount (being one design parameter) and indirectly affect ^{239}Pu generation.

3.3.2. Enrichment

A reduction on ^{239}Pu production is always desirable as follows from Section 3.3 in order to reduce FTC. Fig. 13 shows the ^{239}Pu content against burnup for different enrichment grades. Two observations can be made on that figure:

- The higher the ^{235}U enrichment the slower the ^{239}Pu generation rate. This can be explained by the reduction in neutron flux necessary to keep constant power while increasing the fission cross section.
- The higher the ^{235}U enrichment the higher the final ^{239}Pu content. This can be explained by the spectrum hardening that follows an enrichment increase and considering Eq. (4). The spectrum hardening with the increase of enrichment relies on the fact that fewer thermal neutrons are needed to achieve the same fission rate.

On one hand, an enrichment increase initially reduces ^{239}Pu generation up to about 8000 MWd/tonU, and beyond that burnup, ^{239}Pu build up is increased with the use of higher enrichment (as can be seen in Fig. 13). On the other hand the achievable fuel burnup is increased with higher enrichments.

The calculations made show that the latter effect is more important, resulting in a slight increase in the final ^{239}Pu content due to higher enrichment, and so does the maximum FTC, as can be seen on Fig. 14, where the coefficients are shown up to the burnup levels they can achieve according to Eq. (2). The meaning of the "Equal Cost" dots of Fig. 14 is explained in Section 3.3.4. It can be concluded from Fig. 14 that an enrichment increase produces an increase in the maximum FTC (at EOL) and that the core averaged (or burnup averaged) FTC, defined in Eq. (5), shows only a minimal up-trend with enrichment.

$$FTC_{Avrg} = \frac{\int FTC\, d\mathrm{Bu}}{\int d\mathrm{Bu}} \tag{5}$$

Taking into account the two mentioned effects of an enrichment increase on the FTC, namely, the reduction on the ^{239}Pu generation rate and the increase on the burnup achievable by the fuel, which represent opposing effects on FTC, the validation of the neutronics calculations against experimental benchmarks to assess the tools' uncertainties on burnup calculations is emphasized.

3.3.3. Thermal aspects

This work was based on the CARA fuel Bundle, which has two geometrical features of great interest on PC: the number of rods, which being 52 instead of 37 it lowers the linear and surface power densities; and the collapsible cladding which imposes better cooling conditions for the pellet, i.e., better gap conductance, in comparison with the original Atucha II with-standing fuel (CNEA, 1981). As opposed to the studies of the previous sections which dealt with the effects of design changes on the derivatives of reactivity (α_i) with respect to the thermal parameters in Eq. (3), these geometrical features affect the derivatives of those thermal parameters with respect to power.

The lower surface power density implies lower bubbles generation due to subcooled boiling, according to the effect that the Saha and Zuber (Todreas and Kazimi, 1993) correlation for bubbles departure has in Eq. (1). This gives CARA a lower PC when natural uranium without BNA is used as fuel (which has positive α_{void}), and has a near neutral effect when SEU and BNAs are used according to Section 3.2 to achieve a near zero α_{void}.

The lower linear power density and the better gap conductance have the direct effect of giving a lower operation temperature for the pellet. The consequences on reactivity of this can be divided into two:

(a) On one hand, the colder the fuel more negative the FTC, as can be seen in Fig. 15. This is also usually shown for CANDU fuels at BOL (Yonghee, 2012). This gives a bigger negative FTC (or a smaller positive when FTC is positive due to the presence of ^{239}Pu).
(b) But, on the other hand, the lower the linear power density the lower the fuel temperature jump for a given power increase. This gives a smaller either positive or negative reactivity contribution to PC.

The contradiction of these two quantities is that both are factors of the 1st term in Eq. (3). A similar behaviour to that of fresh fuel (Fig. 15) is observed for the FTC at higher burnup levels, when ^{239}Pu concentrations have increased. i.e., the colder the fuel less positive the FTC. In the discussions of PC of Section 4.3 it is studied whether

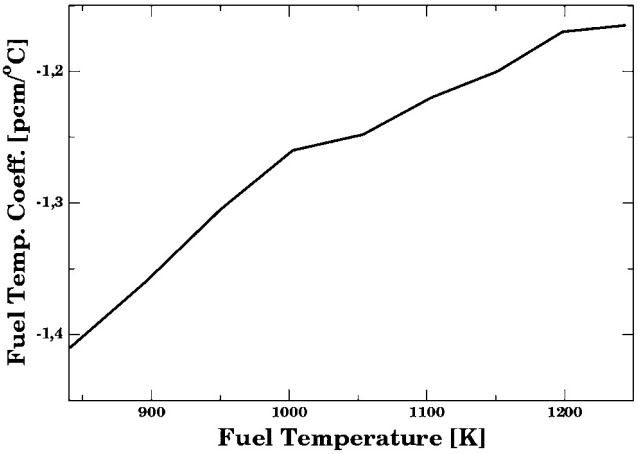

Fig. 15. FTC dependence with fuel temperature for fresh fuel.

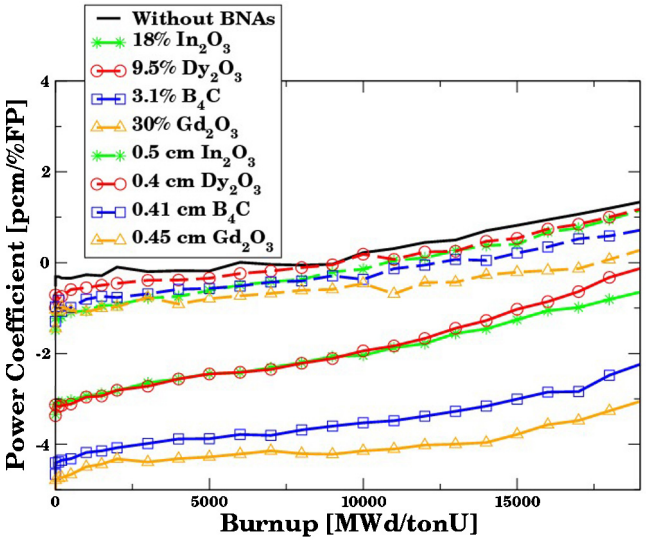

Fig. 16. PC evolution with burnup for different BNAs.

(a) or (b) is more important in changing the PC depending on the burnup.

3.3.4. Economical aspects

Economical aspects can also be studied using the model described in Section 2.3 to reduce the fraction of ^{239}Pu produced in the fuel. The fuel burnup is based on criticality, i.e., the fuel is burned up to a level in which core criticality can no longer be sustained, as expressed in Eq. (2). No other strategy can extract more energy from the fuel in a self-sustained reaction, hence, this strategy leads to the lowest cost (*LUFC*) achievable. The possibility exists, however, of burning the fuel up to economically acceptable burnup levels which could be lower than the burnup levels defined by the criticality criterion.

This is the case for fuels using SEU in HWRs, which *LUFC* is lower than the corresponding to natural uranium, and this cost margin could be used to burn the fuel up to lower levels obtaining as a result a reduction in the ^{239}Pu content and the consequent reduction on the FTC. The "Equal Cost" dots of Fig. 14 show the burnup at which the fuel could be extracted from the core if the same refuelling cost as natural uranium is used as criterion. In Table 4 the burnup, the maximum FTC and the burnup averaged FTC are presented for both, the criticality and the equal refuelling cost criteria, for different enrichments.

These results, however, are only presented to illustrate the effectiveness of the proposed method. It has to be said that, in order to apply this method, it should be done jointly with BNAs addition to maintain reasonable levels of excess reactivity in a core with increased enrichment but with a burnup level that has not been increased accordingly. Besides, it should be noticed that any burnup level lying between those levels of the two criteria mentioned is also a feasible option, complying with both, criticality and economical restraints.

4. Design modifications

Design modifications to CARA fuel were studied on the base of PC, where the different variables such as enrichment level and distribution, BNA type and amount, geometrical characteristics and burnup level at EOL affect each term of Eq. (3) as studied above. How all these effects combine together to form the PC and how they can be used in an optimal design is explained here.

4.1. Burnable neutronic absorbers

An example of the effects of the four BNAs studied in this work is shown in Fig. 16. The curves named with a percentage refer to poisoning of the four inner rods, adding a fraction of BNA to pellets of depleted uranium. The curves named with a length refer to the BNA in pure state in two rods of the mentioned radius, completing the four inner rods of the geometry with two depleted uranium rods.

A reduction on PC is observed for all the BNAs and a clear advantage is seen when the absorbers are mixed with the UO_2 instead of being pure in a separate rod. This advantage is in part due to the effect mentioned in Section 3.3.1b.

Table 4
Reduction in the FTCs as a consequence of burning the fuel with the *Equal Cost* criterion instead of the *criticality* criterion, for a SEU CARA fuel.

Enrichment [wt%]	Burnup [MWd/tonU]		Maximum FTC [pcm/°C]		Average TC [pcm/°C]	
	Crity.[a]	Eq. Cost[b]	Crity.	Eq. Cost	Crity.	Eq. Cost
0.711	7600	7600	−0.013	−0.013	−0.40	−0.40
0.8	11,600	8300	0.23	−0.099	−0.33	−0.49
1.0	18,600	9800	0.50	−0.29	−0.28	−0.61
1.2	24,800	11,600	0.70	−0.422	−0.23	−0.71
1.4	30,600	13,700	0.86	−0.46	−0.20	−0.75
1.6	36,000	15,300	0.97	−0.53	−0.19	−0.80
1.8	41,000	17,300	1.07	−0.59	−0.15	−0.83
2.0	46,000	19,800	1.15	−0.58	−0.13	−0.83

[a] *Crity.* corresponds to values obtained when the criticality criterion was used for burnup level determination.
[b] *Eq. Cost* corresponds to values obtained when the equal refuelling cost criterion was used for burnup level determination.

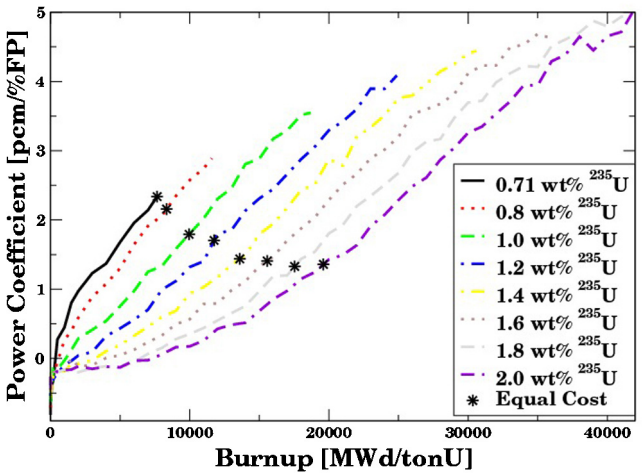

Fig. 17. PC evolution with burnup for different enrichment levels.

4.2. Enrichment

In Fig. 17 the effect of higher enrichment levels in the PC is shown. The behaviour is very similar to that of FTC, but all the values are higher due to the VC, which is positive because the results correspond to a fuel without BNA.

It can be seen in Fig. 17 that an enrichment increase lowers the slope but rises the maximum (final) PC and calculations show that also the average PC is increased. It must be noticed that the maximum PC cannot be negative even using the equal refuelling cost criterion for fuel burnup level determination. Hence, the use of BNAs is mandatory to achieve a negative PC during the whole fuel in-core life.

4.3. Thermal aspects

As mentioned in Section 3.3.3 the geometrical features of CARA fuel lead to a colder fuel, which in turn implies greater (more negative) FTC but at the same time a smaller temperature jump for a given power increase, which counteracts the former effect. In Fig. 18 it is shown how the conductance across the gap affects the PC. It can be seen that a thinner gap, which implies better conductance and colder fuel pellet but less temperature jump with power, does not imply a safer PC at BOL but does imply a safer PC for burnup levels higher than about 4000 MWd/tonU. This can be explained by the fact that the effect (*b*) mentioned in Section 3.3.3 is stronger than effect (*a*). Observing burnup-averaged values of the PC it can be concluded that a colder fuel rod leads to more positive PC when averaged up to 7000 MWd/tonU, but leads to less positive PC when averaged up to 19,000 MWd/tonU.

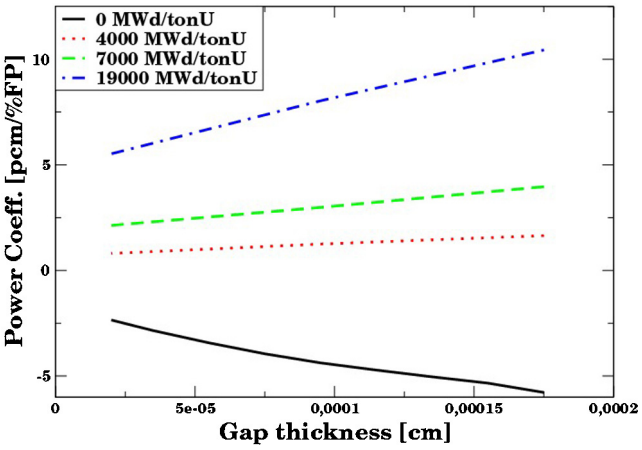

Fig. 18. Influence of the fuel rod gas gap thickness on the PC for different burnup levels.

Table 5
Variables and ranges explored in the optimization.

Variable	Range
Enrichment	0.35–2.4%
BNA type	Dy_2O_3, In_2O_3, B_4C and Gd_2O_3, both, mixed with UO_2 in four central rods, or pure in two central rods
BNA amounts when mixed	0–40%
BNA rod radius when pure	0.1–0.5 cm

4.4. Optimization

The optimization of the enrichment level and distribution, the BNA type and amount and the extraction burnup of the fuel, minimizing the refuelling costs, the power coefficient of reactivity and the power peaking factor was made using computational power, studying a wide range of combination of the involved parameters, shown in Table 5. The discretization used lead to more than 100,000 configurations studied and the optimization results are shown in Tables 6 and 7.

In Table 6 the geometrical and the composition specifications are presented of four fuels: the original Atucha II fuel; CARA fuel with natural uranium; CARA fuel optimized for negative PC, low PPF and minimum refuelling cost; and CARA fuel optimized for a negative PC with low enrichment and low BNA content, with the reference refuelling cost.

In Table 7 the neutronic characteristics of those fuels are presented: PPF, extraction burnup, cost, power and fuel temperature coefficients, and void reactivity. For the power coefficient the average and maximum values are presented, which affect global and local stability, respectively, according to the discussion presented in Section 2.4.3. Some differences can be easily observed from that table. CARA with natural uranium has a smaller maximum PC and a very similar average PC to that of Atucha II. This is due to less bubbles formation as a consequence of a lower surface heat, on one hand, and due to a colder fuel, which gives a less negative FTC at BOL and nearly no difference at EOL (7600 MWd/tonU), on the other hand. In a row of grey colour, the neutronic characteristics are given for this fuel when the extraction burnup is determined so as to achieve the same cost as the reference fuel. A further reduction in FTC and PC is observed, however, the excess reactivity of a core using this fuel would be greater than the design value.

CARA Optimum Cost is the optimum fuel to achieve a negative maximum PC with the lowest cost. The Criticality criterion was used to determine its extraction burnup. Should the equal refuelling cost criterion be used, a more negative either maximum or average PC would be obtained, which is shown in grey. Dy_2O_3 and B_4C also achieved good performance configurations as can be expected from Fig. 16, however, In_2O_3 lead to the most economic. A brief comparison of the achievable costs is shown in Table 8. The fuels compared in Table 8 also differ in the PPF.

And finally, *CARA Low Enrichment* shows a marginally negative maximum PC achieved by limiting the ^{239}Pu build up with the extraction burnup defined by the equal refuelling cost criterion. The excess reactivity was compensated with the addition of extra BNA and this made both criteria of extraction burnup coincident: the burnup that makes the reactor subcritical also corresponds to the reference cost. This configuration that made full use of the cost margin to reduce the ^{239}Pu production has some advantages over the other designs mentioned:

Table 6
Fuel specifications. Results of multidimensional optimization.

Fuel	1st ring of rods		2nd ring of rods		3rd ring of rods		4th ring of rods	
	# rods	Enrichment	# rods	Enrichment	# rods	Enrichment	# rods	Enrichment
Atucha II	1	0.71	6	0.71	12	0.71	18	0.71
CARA U^{nat}	4	0.71	10	0.71	16	0.71	22	0.71
CARA optimum cost	4	$U^{Depl.}$ + 14.5% In_2O_3	10	1.2	16	2.4	22	1.9
CARA low enrichment	2 + 2	$U^{Depl.}$ & Gd_2O_3	10	1.15	16	1.7	22	1.75

Table 7
Fuel characteristics. Results of multidimensional optimization.

Fuel	Criterion	PPF	Burnup [MWd/tonU]	LUFC [mills/kWh]	Max PC [pcm/%FP]	Avg PC [pcm/%FP]	FTC [pcm/°C]	CVR [pcm]
Atucha II	Crit[a]	1.11	7460	8.27	3.43	1.26	0.2	1500
CARA U^{nat}	Crit[a]	1.12	7661	5.63	2.14	1.24	−0.06	1700
	E.C.[b]	1.12	5225	8.27	1.68	1.03	−0.27	1700
CARA optimum cost	Crit[a]	1.26	20600	4.98	−0.02	−1.44	−0.24	180
	E.C.[b]	1.26	12400	8.27	−1.45	−1.95	−0.8	130
CARA low enrichment	Crit[a] = E.C.[b]	1.29	10500	8.27	−0.05	−0.46	0.28	46

[a] *Crit* corresponds to values obtained when the criticality criterion was used for burnup level determination.
[b] *E.C.* corresponds to values obtained when the equal refuelling cost criterion was used for burnup level determination.

Table 8
Comparison of the lowest costs achieved for the different BNAs.

BNA	State	Lowest cost achieving negative PC [pcm/%FP]
Dy_2O_3	Mixed w/UO_2	5.2
	Pure in 2 rods	6.36
In_2O_3	Mixed w/UO_2	4.25
	Pure in 2 rods	8.53
Gd_2O_3	Mixed w/UO_2	7.07
	Pure in 2 rods	5.95
B_4C	Mixed w/UO_2	5.7
	Pure in 2 rods	6.35

- the enrichment is lower than 1.8% at any rod;
- the BNA is pure, which excludes the need for co-sintering UO_2 and BNA;
- the BNA is Gd_2O_3, the most used BNA in the nuclear industry.

All three advantages imply simplicity, hence the design is robust. The relaxation of any of these points allows to achieve a lower cost and a more negative PC.

5. Conclusions

- A deep study of power coefficient was made and its dependence with neutronic, thermal, geometrical and even economical aspects was revealed. The modelling of all these aspects together allowed a consistent and robust approach to optimize the fuel.
- The power coefficient can be reduced by means of reducing the main reactivity components that are thermally coupled: coolant void coefficient and fuel temperature coefficient. The former is reduced by poisoning the inner rods of the fuel bundle and by defining an enrichment grade distribution that simultaneously establishes a K_{inf} radial distribution (as explained in section 3.2), lowers the cost and lowers the power peaking factor. The fuel temperature coefficient is mainly reduced by limiting the ^{239}Pu content by means of poisoning the fuel with neutronic absorbers, rising the enrichment and at the same time redefining the burnup at which the fuel has to be extracted from the core.
- The optimization of the neutronic absorber type and amount, the enrichment grade and distribution, and the extraction burnup of the fuel minimizing the refuelling costs, the power coefficient of reactivity and the power peaking factor was made studying a big number of configurations, the results being two selected designs presented in Tables 6 and 7. One design presents a power coefficient that remains negative during the whole in-core life of the fuel with a considerable advantage on refuelling cost, using a uranium enrichment of up to 2.4%. The other design has no refuelling cost benefit, but achieves a whole life marginally negative power coefficient with lower enrichment and poisoning than the previous design. The optimization methodology allowed to find other configurations with other neutronic absorbers that showed feasibility as well, however the two mentioned were superior in at least one feature. Amongst these configurations some present the neutronic absorber pure in separate rods, without fissile material.
- The focus of this work was on the fuel assembly. However, some of the models developed showed evidence of alternatives to reduce the power coefficient that would involve plant operation changes that might be studied in future work. Such alternatives are: to rise the lower limit of the operating pressure band, reducing as a consequence the bubbles formation and its positive reactivity associated; to lower the coolant channel outlet temperature, which would also require more complex thermal and economical models to assess its effect on the turbine efficiency and the plant operation cost; and to produce an axial power redistribution, producing more power in the lower part and less power in the upper part, reducing in this way the bubbles formation.
- The VC is a very important parameter for safety, and it has been reduced as a mean of reducing PC. The fuel designs presented as alternatives to the original fuel have values smaller than β, the fraction of delayed neutrons, which defines the reactivity needed for prompt-criticality. The VC values achieved and presented in Table 7 are much smaller than that of the original fuel.
- The argentinian nuclear industry has already faced the challenge of changing a PHWR fuel using slightly enriched uranium. The result of such experience being more than a decade of successful operation with reduced fuel costs (NASA S.A., 2002). Should the political decision be made of reducing the power coefficient of reactivity in Atucha II, still much work would be ahead.

Acknowledgements

To Claudio D'Ovidio for his strong support in different aspects of this work. To Armando Marino, for his great help and collaboration in the pellet cladding thermo-mechanical model.

References

Bell, G.I., Glasstone, S., 1970a. Xenon-induced power oscillations. In: Bell, G.I., Glasstone, S. (Eds.), Nuclear Reactor Theory. Van Nostrand Reinhold Company, USA, pp. 555–562.

Bell, G.I., Glasstone, S., 1970b. The experimental boiling water reactor. In: Bell, G.I., Glasstone, S. (Eds.), Nuclear Reactor Theory. Van Nostrand Reinhold Company, USA, pp. 516–517.

Brasnarof, D.O., Marino, A.C., Florido, P.C., Bergallo, J., Daverio, H., González, H., Ghiselli, A.M., Troiani, H.E., Muñoz, C., Bianchi, D., Banchick, D., Giorgis, M., Markiewicz, M., 2005a. CARA development, an argentinean fuel cycle challenge. In: 9th International Conference on CANDU fuel "Fuelling a Clean Future", Ramada Inn on the Bay, Belleville, Canada, September 17–21.

Brasnarof, D.O., Bergallo, J.E., Marino, A.C., Florido, P.C., Markiewics, M., Daverio, H., González, H., 2005b. CARA fuel assembly development. In: Structural Behavior of Fuel Assemblies for Water Cooled Reactors. IAEA.

Budynas-Nisbett, 2006. Mechanical Engineering: Shigley's Mechanical Engineering Design, 8th ed. McGraw Hill, USA.

CNEA, 1979. AECL, 600 MWe CANDU-PHW Central nuclear en Embalse, Cordoba: for Comisión Nacional de Energía Atómica: Preliminary Safety Report.

CNEA, 1981. Preliminary Safety Analysis Report – Atucha II Nuclear Power Plant.

CNSC, 2007. Actuation of Both Shutdown Systems at Point Lepreau, Annual CNSC Staff Report for 2007 on the Safety Performance of the Canadian Nuclear Power Industry, http://nuclearsafety.gc.ca/eng/readingroom/reports/powerindustry/2007/e.cfm (accessed 2013).

DOE, 1980. Heavy Water Reactors Preliminary Safety and Environmental Information Document. Volumen II. DOE/NE 0003.

Driscoll, M.J., Downar, T.J., Pilat, E.E., 1990. The Linear Reactivity Model for Nuclear Fuel Management. American Nuclear Society, USA.

Gyuhong, R., Yonghee, K., Nam Zin, C., 2011. Improvement of power coefficient by using burnable poison in the CANDU reactor. Nuclear Engineering And Design [serial online]. n.d. 241(ICONE-17: Heavy Liquid Metal Technologies and Material Challenges for Gen IV Fast Reactors), pp. 1565–1578.

Hagrman, D.L., Reymann, G.A., 1979. MATPRO Version 11: A Handbook for Materials Properties for use in the Analysis of Light Water Reactor Fuel Rod Behavior. Department of Energy, USA.

IAEA TECDOC 1575, 2008. INPRO Manual on Economics: Guidance for the Application of an Assessment Methodology for Innovative Nuclear Energy Systems. IAEA, Austria.

http.//www-nds.iaea.org/wimsd/downloads.htm (accessed 2013).

http://www.relap.com/ (accessed 2013).

Johansson, E., 1987. Comparison of calculated and measured reactivity coefficients for light water reactor lattices. In: IAEA TECDOC 491, Nuclear Data for the Calculation of Thermal Reactor Reactivity Coefficients, Austria.

KAERI, 2001. Assessment CANDU Physics Codes Using Experimental Data – Part I: Criticality Measurement, KAERI/TR-1925/2001.

Kay, R.E., 1976. Lattice Measurements with 37-Element Bruce Reactor Fuel in Heavy Water Moderator: Detailed Lattice Cell Parameters. Chalk River Nuclear Laboratories.

Knott, D., Yamamoto, A., 2010. Lattice physics computations. In: Gabriel, D. (Ed.), Handbook of Nuclear Engineering, Volume I: Nuclear Engineering Fundamentals. Springer, Germany.

Lepp, R.M., Frketich, G., 1979. Two Phase Control Absorber Development Program: Closed Loop Control Experiments and Noise Measurements in the ZED-2 Test Reactor, AECL 6089.

Lestani, H., Florido, P., González, H., 2011a. Conceptual Engineering of CARA Fuel Element with Negative Void Coefficient for Atucha II. Science and Technology of Nuclear Installations.

Lestani, H., Florido, P., González, J., 2011b. Reactivity coefficients dependence with burnup. In: International Workshop on Burnup Credit Criticality Calculations Methods and Applications, Beijing, China, 25–28 October 2011, Proceedings to be published on IAEA site soon.

Lewis, E.E., 1977. Nuclear Power Reactor Safety. John Wiley and Sons, New York.

Marino, A.C., 2011. Starting Point, Keys and Milestones of a Computer Code for the Simulation of the Behaviour of a Nuclear Fuel Rod, Science and Technology of Nuclear Installations, Volume 2011, Article ID 326948 (Ref.: http://www.hindawi.com/journals/stni/2011/326948/)

Mazzantini, O., Schivo, M., Di Césare, J., Garbero, R., Rivero, M., Theler, G., 2011. A Coupled Calculation Suite for Atucha II Operational Transients Analysis. Science and Technology of Nuclear Installations.

McDonnel, F.N., Green, R.E., 1978. Spatial power control in large CANDU reactors: the whys and wherefores. In: 18th Annual International Conference of the Canadian Nuclear Association, Ottawa.

http.//www.cnea.gov.ar/xxi/para-conocer/atucha/uranio-enriquecido.asp.2002.

NPCIL, 1995. Pressurized heavy water reactor PHWR-500 system description and development status. In: IAEA-TECDOC-881: Design and Development Status of Small and Medium Reactor Systems.

http://www.parl.gc.ca/HousePublications/Publication.aspx?DocId=4009510 (accessed February, 2013).

Rahnema, F., Gheorghiu, H.N.M., 1996. ENDF/B-VI benchmark calculations for the Doppler coefficient of reactivity. Ann. Nucl. Energy 23 (12), 1011–1019.

Todreas, N.E., Kazimi, M.S., 1993. Nuclear Systems I: Thermal Hydraulic Fundamentals. Taylor & Francis, USA.

Tong, L.S., Weisman, J., 1996. Thermal Analysis of Pressurized Water Reactor, 2nd ed. American Nuclear Society, United States.

Ward, A.M., Collins, B.S., Madariaga, M., Xu, Y., Downar, T.J., 2011. Methods and Model Development for Coupled RELAP5/PARCS Analysis of the Atucha-II Nuclear Power Plant. Science and Technology of Nuclear Installations.

Yonghee, K., 2012. Monte Carlo re-evaluation of CANDU-6 physics parameters. In: IAEA Workshop on Advanced Code Suite for Design, Safety Analysis and Operation of HWRs, Ottawa, Canada, October 2–5.